Akademia Górniczo-Hutnicza im. Stanisława Staszica w Krakowie

Wydział Informatyki

Praca dyplomowa

Planar segment-based global localization for autonomous agents

Globalna lokalizacja agenta w oparciu o segmenty płaszczyzn

Autor: **Jan Rodzoń**
Kierunek: **Informatyka**
Opiekun pracy: **prof dr hab. inż. Bogdan Kwolek**

Kraków, 2024

Składam szczególne podziękowania mojemu Promotorowi, prof. dr hab. inż. Bogdanowi Kwolek za życzliwość, wszechstronne wsparcie, cierpliwość, cenne uwagi merytoryczne oraz poświęcony czas.

Streszczenie

Niniejsza praca bada obecne rozwiązania i architektury sieci neuronowych pod kątem lokalizacji agenta w oparciu o rozpoznawanie segmentów płaszczyzn na zdjęciach RGB. W ramach pracy wybrano oraz sprawdzono zastosowanie kilku najnowszych technologii opartych o sieci neuronowe w radzeniu sobie z rozpoznawaniem segmentów płaszczyzn w różnych warunkach życia codziennego.

Abstract

This thesis examines current neural network solutions and architectures in terms of agent localization based on recognition of plane segments from RGB images. The work selects and tests the application of several state-of-the-art technologies based on neural networks in dealing with the recognition of plane segments in various everyday conditions.

Contents

List of Figures

List of Tables

List of Listings

1. Preface

We live in the era of automation. Everywhere robots are taking over the positions, which require not only repetitive actions but also more complicated tasks. In this environment, there are more and more machines that are operating within some contained spaces like commercial buildings or warehouses. There is also a growing market for indoor drone usage. Because of that, there is a need for a means of autonomous localization of these machines, which we will call generically agents in this work. Recent advances in computer vision and artificial intelligence come in handy and provide some models for localization based on planar segments.

1.1. Motivation

Unfortunately, when one tries to use or apply the latest state-of-the-art models and algorithms there are a lot of obstacles to it—starting from missing environment requirements, through outdated libraries, which have dropped backward compatibility, and finishing on overfitted models, which are good only within specific circumstances and are not applicable in ordinary indoor applications. This thesis aims to contribute to the field of agent localization and plane segmentation by reviewing the current development of plane segmentation and measuring its potential on data that is completely different from the training or testing one. Additionally, some of the latest models are difficult to get started. In this work, I also try to ease the workload required to get these projects going for future contributors or researchers.

1.2. Content of this work

The thesis is organized into chapters as follows:

- **Chapter 2: Plane Segmentation Development** 2

  It reviews different approaches to plane segmentation, including first attempts and new developments.

- **Chapter 3: Thesis aims** 3

  It lists the objectives set for this work.

- **Chapter 4: Implementation** 4

  It describes the initiation and operation of selected projects, including encountered problems and implemented solutions.

- **Chapter 5: Results Evaluation** 5

  It presents and compares the results obtained from selected models and discusses their usefulness in everyday situations.

- **Chapter 6: Conclusions** 6

  It summarises the results obtained in this work and shows potential directions for future research.

2. Plane Segmentation Development

2.1. RGB-D Approach

In the previous century, it was almost unimaginable to parse the film in real time and interpret the frames. Furthermore, the depth component seemed necessary to find plane segments in the pictures. Since the RBG-Depth (RGB-D) sensors were only available in the form of expensive machines like time-of-flight cameras or scanning 3-D laser range finders, [1] there were no possibilities for a broad usage of this technology, and thus, it saw little interest. Nevertheless, there were several approaches for recognizing planar sections in the pictures.

2.1.1. Rabbani Classification

Rabbani [2] categorized contemporaneous plane segmentation algorithms into three main categories:

1. **Edge-based segmentation**

   This approach comprises two stages:

   - Edge detection

     It involves scanning the depth map for points in which there are some changes in the local surface properties (like gradients or normals) above a designated threshold.

   - Point grouping

     This part groups together points inside borders detected in the previous step.

   One of the first successful applications of this method was done by Bhanu et al. [3] Another more recent work with promising results was published by Sappa et al. [4]

2. **Surface-based segmentation**

   Algorithms of this type try to merge points with similar local surface properties. Generally, there are two approaches:

- Bottom-up

  It begins with selecting starting points and expanding from them using some predefined similarities. It is worth noting that choosing these initial points is crucial as the results depend on them - i.e., you do not find segments without starting points within them.

- Top-down

  It starts by associating one big plane with all of the points in the picture. Then, it cuts it into smaller pieces until it achieves a predefined fitting threshold.

One of the most prominent uses of this approach was published by Xiang et al. [5]. They utilized the bottom-up approach, which generally is used much more often than the top-down technique.

3. **Scanline-based segmentation**

   This approach treats rows or columns of pixels as scanlines. It takes advantage of the fact that each scanline projection over a 3D surface creates a 3D line. Ultimately, the technique consists of two stages:

   - Line segments extraction

     This stage involves processing scanlines to find line segments.

   - Line segments grouping

     In this step, the extracted line segments are grouped with the neighbouring ones based on their similar surface properties to form plane segments.

   One of the first publications regarding this technique was made by Jiang et al. [6], giving a groundbreaking performance at the time. Natonek [7] utilized a similar approach for robots just two years later, having promising results.

These various techniques tackled plane segmentation from different perspectives. However, most implementations required a large amount of computation, thus rendering them inconvenient for real-time agent localization due to the inability to process multiple frames per second.

2.1.2. RGB-D Affordability

Plane segmentation started drawing more attention at the beginning of the 2010s when inexpensive RGB-D sensors (e.g. Microsoft Kinect) became available [1]. With the lower price came higher availability and more research. Multiple algorithms were developed at that time. They included different variations of plane extraction from the depth property with various optimisations, among others:

- By Taguchi et al. [8] - one that successfully uses Simultaneous Location and Mapping (SLAM) with a Kinect 3D sensor. It contains the Random Sample Consensus (RANSAC) [9] - a widely used technique in the Point Cloud Library (PCL) [10];
- By Salas-Moreno et al. [11] - one that uses Principal Component Analysis (PCA) to find plane candidates;
- By Michael Kaes [12] - one that uses infinite planes and least-squares for mapping, combined with minimal representation;
- By Hsiao et al. [13] - one that uses a keyframe-based approach and is viable on Central Processing Unit (CPU)-only devices.

All of them utilize some variation of plane extraction from the depth property with a veraiety of optimizations.

2.1.3. RGB-D To Point Cloud Mapping

For every RGB-D algorithm, it is essential to correctly calculate the real point coordinates based on the pixel location in the image. The results map the factual world as seen by the camera. The computation includes the focal length and the principal point (often the image centre) and requires camera intrinsic parameters.

In the first step, the camera matrix (C) is determined:

$$C = \begin{bmatrix} f_x & 0 & c_x \\ 0 & f_y & c_y \\ 0 & 0 & 1 \end{bmatrix} \tag{2.1}$$

where:

- f_x is the focal length on x-axis
- f_y is the focal length on y-axis
- c_x is the principal point x-axis coordinate
- c_y is the principal point y-axis coordinate

Then, for each pixel with 2D coordinates $p(u, v)$ the world point $P(\mathbf{X}, \mathbf{Y}, \mathbf{Z})$ can be calculated as follows:

$$\begin{cases} \mathbf{X} = \frac{(u-c_x)\cdot\mathbf{Z}}{f_x} \\ \mathbf{Y} = \frac{(u-c_x)\cdot\mathbf{Z}}{f_x} \\ \mathbf{Z} = d_p \end{cases} \tag{2.2}$$

where:

- d is the depth component in RGB-D image for pixel $p(u, v)$
- u is the pixel p x-axis coordinate
- v is the pixel p y-axis coordinate

Figure 2.1 presents a visual explanation of the pixel projection mapping described above.

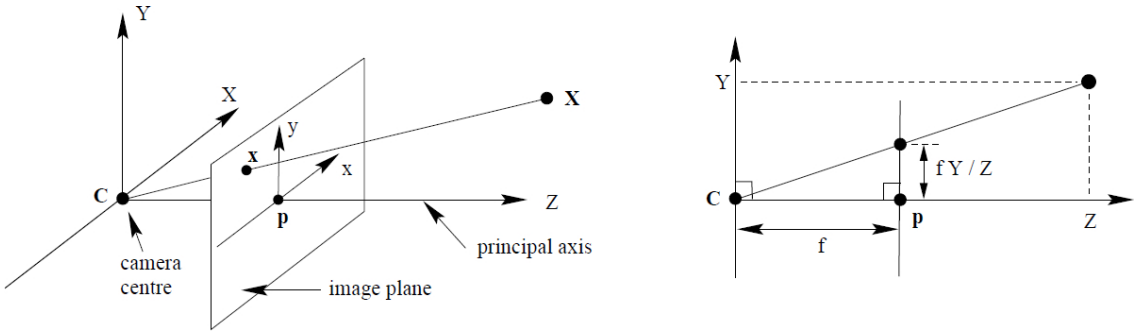

Figure 2.1.: Pinhole Camera Model pixel projection. [14]

A set of 3D points, called Point Cloud, is obtained from the computation [15]. Points in the cloud are organized, therefore, adjacent points correspond to real neighbouring locations. Consequently, the memory layout uses the same order, which speeds up the steps of many algorithms, like searching for nearest neighbours.

2.1.4. RGB-D State of the art

One of the most successful algorithms developed using the RGB-D technique is published by Zhang [1] et al. discussed in more detail in the following chapter. Their technique is based on scanlines. The high-level overview of the algorithm can be seen in the Figure 2.2.

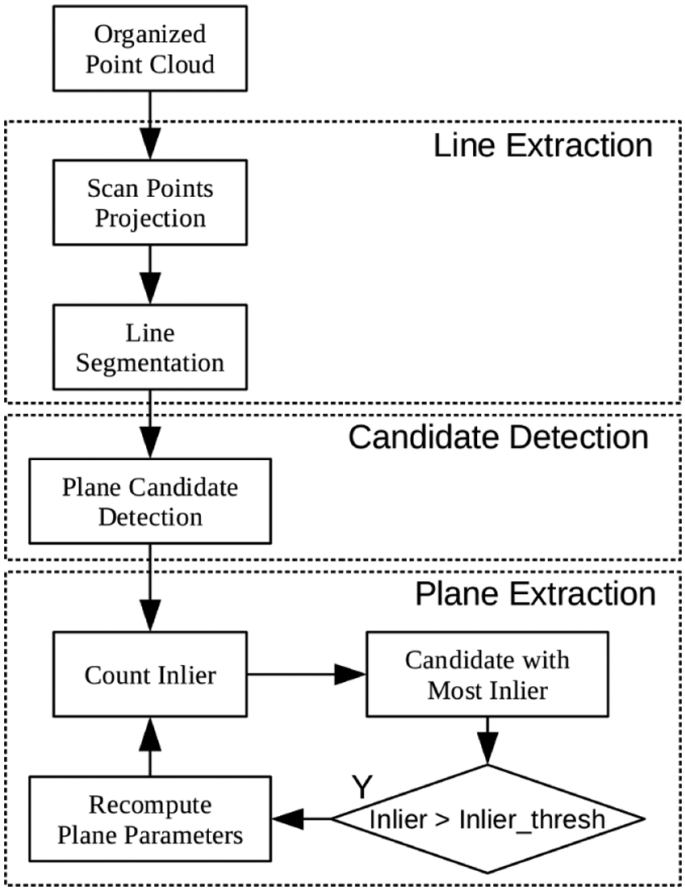

Figure 2.2.: Flowchart of the plane segmentation approach. [1]

There are three main stages of the algorithm:

1. **Line Extraction**

   The method, instead of looking for line segments on all possible scanlines, selects a few scanlines periodically, e.g., every thirty rows. It is worth mentioning that it is possible to select either rows or columns, and we can adjust the interval size to achieve a compromise between accuracy and performance.

   - Scan Points Projection

     Each selected line is treated as a 2D laser scan for the purpose of segmentation. Then, for each pixel on these lines, the projection is calculated according to the equation 2.2 from the RGB-D To Point Cloud Mapping section. 2.1.3

- Line Segmentation

  To extract line segments, the following algorithm is used:

  Algorithm 1: Line Regression [1]

  1 Initialize sliding window size N_f.
  2 Fit a line to every N_f consecutive points.
  3 Compute a line fidelity array. Each element of the array contains the sum of Mahalanobis distances between every three adjacent windows.
  4 Construct line segments by scanning the fidelity array for consecutive elements having values less than a threshold.
  5 Merge overlapped line segments and recompute line parameters for each segment.

  This algorithm was initially proposed in a study by Arras and Siegwart. [16] It yielded good results without much computational complexity.

2. **Plane Candidate Detection**

   For each line segment, a plane candidate is calculated in the following way:

   - Selection of points for local normals

     The more points are selected, the more accurate the result, but with the cost of computational complexity. The middle point for each line segment is a good compromise, which is confirmed empirically in the article.

   - Calculation of local normals

     For each selected point, the smoothing region is chosen as a square with a fixed size (for example 20 pixels). Then, for each region, the principal component analysis (PCA [17]) algorithm is executed, which gives us the local normal.

   - Selection of plane candidates

     Lastly, the valid points regarding PCA are chosen as an inlier (part of the plane) from the smoothing region. Then, the local curvature is calculated, and the inliers with the normals with curvature less than a maximum threshold are selected as plane candidates.

   Example plane candidates result can be seen in the Figure 2.3

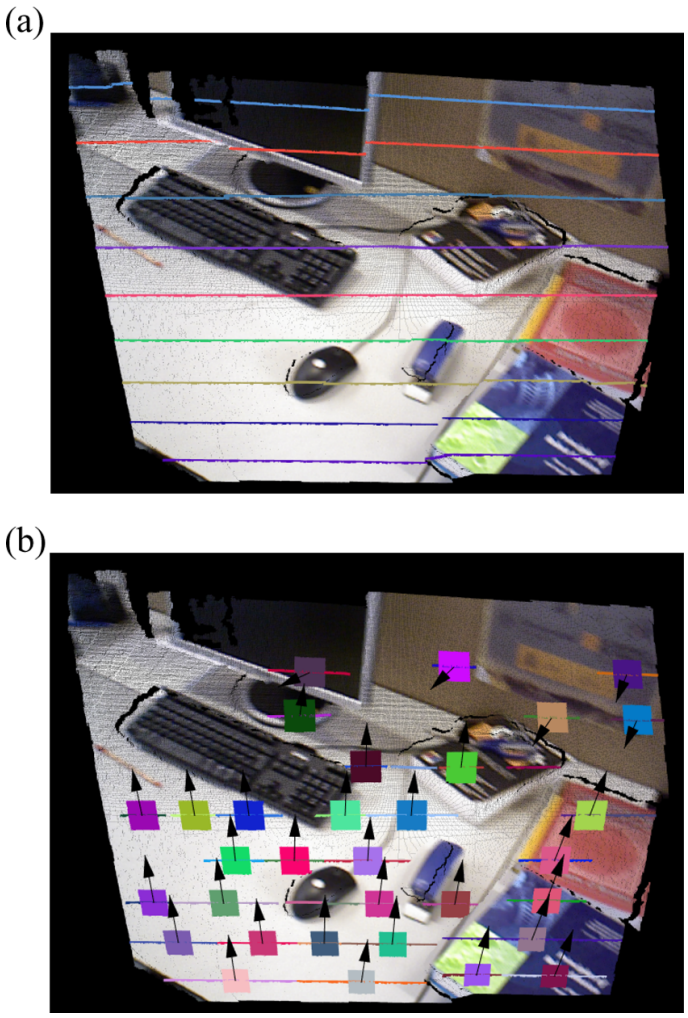

Figure 2.3.: Examle showing plane candidates calculation. [1] (a) Colored lines are scanlines (b) Each plane candidate is represented by part of the line segment (colored line), normal smoothing region (colored square) and local normal emerging from the middle point (black arrow)

3. **Plane Extraction**

   For plane extraction, the recursive algorithm is used, which is presented in the Algorithm 2 It takes every plane candidate and discards each with its inlier N_s smaller than the minimal threshold $N_{sthresh}$. Then, it calculates the quality of the inlier by counting how many neighbours within range d_n are closer to the plane than a distance threshold d_τ. The candidate is also invalidated if the number of valid points is smaller than the minimal threshold $N_{\xi_{thresh}}$.

Next, the biggest approved inlier $N_{\xi_{max}}$ is considered to be part of the plane segment from the final result. Ultimately, principal component analysis [17] is calculated again for the selected candidate $N_{\xi_{max}}$, and the actual inlier of the chosen plane segment is deducted directly from the point cloud. After adding the plane segment to the result set, the plane candidate $N_{\xi_{max}}$ is removed from the possibilities for the next iterations. This sequence of actions is repeated recursively until there are no valid plane candidates.

Algorithm 2: Recursive plane extraction [1]

Input: plane candidates $\hat{\xi}_i, i = 1, 2, \cdots, n$.
Output: plane segments $\xi_j, j = 1, 2, \cdots, m$.

while *number of valid plane candidates* $\neq 0$ **do**
  initialize maximum inlier number $N_{\hat{\xi_{max}}} \leftarrow 0$, corresponding plane parameters $\hat{\xi_{max}} \leftarrow$ *invalid*.
  for $i = 1$ ***to*** n **do**
    if $\hat{\xi}_i$ *is invalid* **then**
      count number of valid points N_s in normal smoothing region
      if $N_s > N_{sthresh}$ **then**
        count number of valid points $N_{\hat{\xi}_i}$ by point-plane distance threshold d_τ and neighbour distance threshold d_n
        if $N_{\hat{\xi}_i} > N_{\hat{\xi_{max}}}$ ***and*** $N_{\hat{\xi}_i} > N_{\hat{\xi_{thresh}}}$ **then**
          $N_{\hat{\xi_{max}}} = N_{\hat{\xi}_i}$
        end
      else
        $\hat{\xi}_i \leftarrow$ *invalid*
      end
    end
  end
  if $N_{\xi_{max}} > N_{\xi_{thresh}}$ **then**
    recompute plane parameter $\hat{\xi_{max}}$ using all the inlier
    save result plane $\xi_j \leftarrow \hat{\xi_{max}}$
    delete inlier in point cloud data
  else
    break
  end
end

2.2. RGB Approach

With the recent boom in artificial intelligence, especially in neural networks, the scientific community has realized, that it is possible to get rid of all depth scanners and extract information about plane segments from simple RGB images, similar to our brain. The first successful attempt using a neural network to detect plane segments from a plain RGB was PlaneNet brought by Liu et al. [18] It took advantage of the recent advancement in neural network technology - Dilated Residual Network (DRM) [19], which was published just a year prior. This success drew much attention to the topic, and since then, there have been multiple enhancements and progressions. Based on the PlaneNet, SlamCraft was introduced by Rambach et al. [20] - a SLAM framework, which proved, that monocular SLAM systems are feasible with adequate neural network untilization. Yu et al. [21] tackled the problem from a different perspective. They have proposed a two-stage algorithm using an encoder-decoder approach and achieved promising results. A big step forward was the introduction of PlaneRCNN by Liu et al. [22] They used mask R-CNN [23] - a recent innovation in a neural network to computer vision. The state-of-the-art advancements are brought by Yaxu Xie et al. in the form of PlaneSegNet [24]. This framework achieves great results and was proved SLAM-worthy by Shy et al. in the form of Structure PLP-SLAM [25], which uses PlaneSegNet for plane segmentation.

2.2.1. Begin: Ask if needed neural network theory

All of the methods addressed in Section 2.2 use some variation of neural networks. Why is that the case? Well, many years ago, Kurt Hornik, Maxwell Stinchcombe, and Halbert White proved mathematically that multilayered feedforward neural networks are universal approximators. [26] So why haven't they been widely spread and entangled in multiple tasks? Training a neural network is highly resource-intensive. To train a neural network, huge amounts of data and computation are required, and thus, the hardware capabilities prevented the scientific community from satisfactory results. With the era of GPUs, the situation has changed and we can see the presence of neural networks almost everywhere. In the section 2.2.2 the basic principles of neural networks are presented.

2.2.2. Neural Networks

2.2.3. End: Ask if needed neural network theory

2.2.4. RGB state-of-the-art - PlaneSegNet

The current state-of-the-art RGB plane segmentation is represented by PlaneSegNet proposed by Yaxu Xie et al. [24] The architecture is based on the YOLACT++ instance segmentation framework published by Bolya et al. [27] with added optimizations in some of the modules. The general overview of the framework can be seen in Figure 2.4. The architecture is quite complex and consists of:

- Encoder

  Produces a group of multi-scale feature maps P_3, P_4, P_5, P_6, P_7.

  - Backbone Network It is a deep residual network based on the ResNet by He et al. [28]
  - Feature Pyramid Feature Pyramid Network structure based on the work of Lin et al. [29]

- Residual Feature Augmentation

  Apart from the standard connection, layer C_5 of the backbone is connected to the prediction layer P_5 through the Residual Feature Augmentation brought by Guo et al. [30] It improves the context of the spatial placement of the features.

- Prediction Head For each layer of the Feature Pyramid Network, it produces c class confidences, four bounding box regressors, and k mask coefficients.

- Fast Feature NMS

  The most significant innovation brought by PlaneSegNet. It aims to enhance overlapping instances detection reliability. It is discussed more in detail in the Subsection 2.2.4.

- ProtoNet

  It is a convolutional neural network. It takes the feature maps from the P_3 layer and predicts k channels for prototype masks.

- Mask Assembly

It assembles prototype masks based on the following linear combination equation:

$$M = \sigma(P\mathbf{C_T}) \tag{2.3}$$

where:

- σ is a non-linear sigmoid function
- P is a tensor of dimensions $h \times w \times k$ containing prototype masks
- $\mathbf{C}$ is a matrix of dimensions $n \times k$ containing mask coefficients for the output of Fast Feature NMS 2.2.4

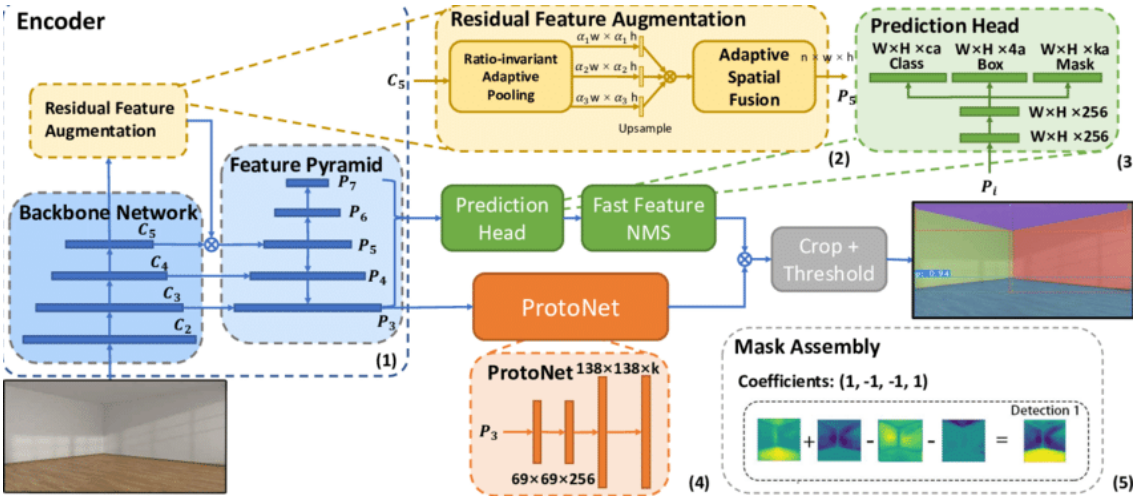

Figure 2.4.: PlaneSegNet Architecture. (1) Encoder (2) Residual Feature Augumentation (3) Prediction Head (4) ProtoNet (5) Mask Assembly [24]

The loss function

It takes into consideration each of the mask, confidence, and bounding box (localization) losses. It is represented with the following equation:

$$\mathscr{L}(x, C, B, M) = \frac{1}{N}(\mathscr{L}_{conf}(x, C) + \alpha\mathscr{L}_{loc}(x, B, B_{gt}) + \beta\mathscr{L}_{mask}(x, M, M_{gt})) \tag{2.4}$$

where:

- C is a confidence representation
- B is a bounding box (localization) representation
- M is a mask representation
- N is the number of positive matchings
- $\mathscr{L}_{conf}$ and $\mathscr{L}_{loc}$ are loss function taken from the single-shot detector presented by Liu et al. [31]
- $\mathscr{L}_{mask}$ is the pixel-wise binary cross entropy between the ground truth and predicted masks.

Fast Feature Non-maximum Suppression

It was observed, that strongly overlapping bounding boxes often don't belong to the same object. Because of that, usage of the classic NMS method brings unnecessary calculation overhead. To resolve this issue, a new method is introduced, Fast Feature Non-maximum Suppression. The technique is based on the research of Salcheider and Niels, who came up with Feature Non-maximum Suppression. [32]

This method is presented in the form of Algorithm 3 The N_1 and N_2 are thresholds for the common area of overlapping bounding boxes (IoU). If IoU is smaller than N_1, the boxes are considered to be from different objects. However, if IoU is bigger than N_2, the boxes are considered to be from the same object. Finally, if IoU is between N_1 and N_2, the similarity S_i of the objects is calculated, and if it is below the given likeness threshold T, the boxes are considered to be from different objects. It is worth noting that this approach adds minimal overhead compared to the Fast NMS.

Algorithm 3: Fast Feature NMS [24]

Input: $P \leftarrow Sort(Proposals)$ with Scores, $D \leftarrow \emptyset$

$X^{triu} \leftarrow GetPairwiseIoU(P)$
$K \leftarrow max(X^{triu})$ column-wise
if $K_i \leqslant N_1$ **then**
    $PUSH(p_i, D)$
else
    if $K_i \leqslant N_2$ **then**
        $C^{triu} \leftarrow GetCosineSim(p, D)$
        $S \leftarrow max(C^{triu})$ column-wise
        if $S_i \leqslant T$ **then**
            $PUSH(p_i, D)$
        end
    end
end
return D

3. Thesis Aims

3.1. Plane Segmentation Real-life Usability

Many technologies claim that their results are unprecedented, with almost endless application possibilities. Indeed, this is often true, but some algorithms or frameworks are tested on specific datasets. This is especially the case for neural-network-based solutions, where the test and train data are extracted from the same dataset. Therefore, when one tries to apply such technology practically and subjects it to completely different data (from the test and train data), it sometimes turns out that the results are not as good as claimed.

I have selected two state-of-the-art methods that use RGB-only data:

1. planercnn [22]
2. PlaneRecNet [33]

Both of these technologies, besides performing plane segmentation, provide depth estimation. This feature can give insight into the particular algorithm's 'understanding' of an image.

4. Implementation

4.1. Working environment

This section describes the working environment from both, software and hardware perspectives.

4.1.1. Technology stack

The following technology stack was used:

- **Ubuntu 20.04** - Linux operating system widely used in the computer vision community. [34]
- **Conda** - Package manager for isolated environments. [35]
- **Python 3.9.18** - Main programming language for writing code and conducting experiments. [36]
- **CUDA 11.7.1** - A development environment for GPU-accelerated applications. [37]
- **PyTorch 1.13.1** - A machine learning framework with CUDA integration. [38]

4.1.2. Workstation parameters

The experiments were prepared and conducted on a personal computer with the following specifications:

- CPU: Intel(R) Core(TM) i5-10400F CPU @ 2.90GHz [39]
- GPU: NVIDIA GeForce RTX 4060 [40]
- Hard Drive: Samsung SSD 990 PRO 2TB [41]

4.2. Preparing test dataset

To evaluate the algorithms' real-life usefulness, I prepared a set of photos of various indoor scenes and outskirts of the building. I shot each scene in two different lighting conditions - day and night. A model for the scenes was the main building of the AGH faculty of Computer Science - D17.

I took pictures using the rear camera of the `Samsung Galaxy A54 5G` phone, model `SM-A546B/DS`. The image resolution is 4080x3060. The horizontal field of view (FoV_h) is 72.7° and the vertical field of view (FoV_v) - 57.8°. [42]

4.2.1. Calculating Camera Matrix

Many plane segmentation algorithms require camera intrinsic parameters to correctly perform plane segmentation and depth prediction. In this thesis, PlaneRCNN required the following camera matrix:

$$C = \begin{bmatrix} f_x & 0 & c_x \\ 0 & f_y & c_y \\ 0 & 0 & 1 \end{bmatrix} \tag{4.1}$$

where:

- f_x is the focal length in pixels on x-axis
- f_y is the focal length in pixels on y-axis
- c_x is the principal point x-axis coordinate in pixels
- c_y is the principal point y-axis coordinate in pixels

Based on the pinhole camera model from Figure 2.1 from Section 2.1.3, these are the mathematical recipes for all the necessary parameters:

$$\begin{cases} f_x = \frac{\frac{1}{2}R_h}{\tan(\frac{1}{2}FoV_h)} \\ f_y = \frac{\frac{1}{2}R_v}{\tan(\frac{1}{2}FoV_v)} \\ c_x = \frac{1}{2}R_h \\ c_y = \frac{1}{2}R_v \end{cases} \tag{4.2}$$

where:

- R_h is the camera horizontal resolution in pixels

- R_v is the camera vertical resolution in pixels
- FoV_h is the camera horizontal field of view in degrees
- FoV_v is the camera vertical field of view in degrees

The image resolution is `4080x3060`, so $R_h = 4080$ and $R_v = 3060$. Fields of view are $FoV_h = 72.7°$ and $FoV_v = 57.8°$. Applying these values to Equation 4.2 gives the following result:

$$\begin{cases} f_x = 2772.05 \approx 2772 \\ f_y = 2771.59 \approx 2772 \\ c_x = 2040 \\ c_y = 1530 \end{cases} \tag{4.3}$$

4.3. Setting-up the environment

The first step in using every repository is setting up the working environment. Nowadays, almost every project using artificial intelligence is Python-oriented, and algorithms incorporating some form of neural networks are no exception. It is not coincidental. The Python environment is rich in multiple sophisticated libraries, providing means for many highly complicated tasks, such as matrix operations, which are essential for any neural network manipulations. Additionally, training a neural network requires immense computation, and graphic cards (Graphic Processing Unit - GPU) are responsible for doing most of it. GPUs have high computing capacity but are conventionally optimized for graphic problems. Thus, separate dedicated drivers are necessary to transform a classic GPU into a General Purpose Graphic Processing Unit (GPGPU) tuned for mathematical calculations.

Ultimately, we end up with a tremendously complicated environment with dedicated graphic drivers, python libraries, system libraries, etc. Each of these components adds a layer of complexity. Taking into consideration the environment specification, getting a state-of-the-art neural network project going may be a highly challenging and time-consuming task.

4.3.1. PlaneRCNN

I started my work with an attempt to set up the PlaneRCNN repository. [43] The provided files seemed complete - an installation instruction followed by a `requirements.txt` file. The installation went smoothly. Next, I tried to run an example evaluation:

```
$ python evaluate.py --methods=f --suffix=warping_refine --
    dataset=inference --customDataFolder=example_images
```

I received an error: GPU software cannot run `nms` - a part of the PlaneRCNN repository.

```
Traceback (most recent call last):
File "evaluate.py", line 20, in <module>
  from models.model import *
File "/home/agent/Masters/Repos/planercnn/models/model.py",
    line 23, in <module>
  from nms.nms_wrapper import nms
File "/home/agent/Masters/Repos/planercnn/nms/nms_wrapper.py
    ", line 11, in <module>
  from nms.pth_nms import pth_nms
File "/home/agent/Masters/Repos/planercnn/nms/pth_nms.py",
    line 2, in <module>
  from ._ext import nms
File "/home/agent/Masters/Repos/planercnn/nms/_ext/nms/
    __init__.py", line 3, in <module>
  from ._nms import lib as _lib, ffi as _ffi
ImportError: /home/agent/Masters/Repos/planercnn/nms/_ext/nms/
    _nms.so: undefined symbol: __cudaRegisterFatBinaryEnd
```

After a thorough investigation, I discovered that the PyTorch [38] in version `0.4.1` supports only old Compute Unified Device Architecture (CUDA) [37] versions, which are incompatible with modern GPUs.

Based on this knowledge, I tried to bump the PyTorch version to at least `1.10`, which supports some of the latest CUDA releases, but I encountered another obstacle. There are two custom CUDA modules written in C [44]:

- `nms` - implementation of Non-Maximum Suppression algorithm
- `roi_align` - implementation of RoIAlign algorithm proposed by He et al. [23]

Unfortunately, PyTorch from version `1.0.0` has removed support for C modules and left only the `C++` [45] option. (it was part of the `torch.legacy` package [46]) Thus, these custom modules needed to be rewritten. After additional research, instead of changing them, I removed them completely, thanks to the publicly available replacement by WeihongPan [47]:

We can get rid of both custom modules:

- `nms` Higher versions of the PyTorch library already provide the Non-Maximum Suppression algorithm, so a version update is enough.

- `roi_align` An implementation of the RoIAlign algorithm is now available as a separate package [48], so it is installed instead of using the custom module.

As a result, setting up the PlaneRCNN environment was simplified.

WeihongPan also published a method of setting up the PlaneRCNN environment. However, the installation failed with an error suggesting package incompatibilities.

It failed with the following error:

```
Collecting cffi==1.15.0 (from -r requirements.txt (line 10))
  Using cached cffi-1.15.0-cp39-cp39-manylinux_2_12_x86_64.
     manylinux2010_x86_64.whl.metadata (1.2 kB)
Collecting numpy==1.19.2 (from -r requirements.txt (line 11)
   )
  Using cached numpy-1.19.2.zip (7.3 MB)
  Installing build dependencies ... done
  Getting requirements to build wheel ... done
  Preparing metadata (pyproject.toml) ... error
  error: subprocess-exited-with-error
  RuntimeError: Running cythonize failed!
```

which suggests package incompatibilities.

On this ground, I decided to select my own set of compatible libraries and ship them as a Conda [35] environment definition. As a result, I created the `environment.yml` file:

```
name: planercnn_pytorch_1_13_cuda_11_7
channels:
  - pytorch
  - conda-forge
  - nvidia
  - defaults
dependencies:
  - cffi=1.15.1
  - matplotlib=3.8.4                # required by RoIAlign test.sh https
      ://github.com/longcw/RoIAlign.pytorch
  - mkl=2024.0                      # due to a pytorch bug https://
      github.com/pytorch/pytorch/issues/123097
  - numpy=1.21.2
  - opencv=4.5.5
  - pytorch::pytorch=1.13.1
  - scikit-image=0.19.3
  - pytorch::torchvision=0.14.1     # required by RoIAlign test.sh https
      ://github.com/longcw/RoIAlign.pytorch
  - tqdm=4.66.5
prefix: $HOME/.conda/envs/planercnn_pytorch_1_13_cuda_11_7
```

Additionally, I prepared a convenience script for RoIAlign installation:

```
#!/bin/bash

WORKDIR="roi_align_installation"
GITHUB_URL="https://github.com/longcw/RoIAlign.pytorch"

mkdir $WORKDIR
git clone $GITHUB_URL $WORKDIR
cd $WORKDIR

python setup.py install
./test.sh

cd ..
rm -rf $WORKDIR
```

As a final step, I added an instruction which sets up the PlaneRCNN in just a few simple steps:

```
$ conda env create -f environment.yml
$ conda activate planercnn_pytorch_1_13_cuda_11_7
$ conda install h5py=3.7.0
$ ./install_roi_align.sh
```

4.3.2. PlaneRecNet

With the PlaneRecNet repository [49], there was a similar situation as with the PlaneRCNN (Section 4.3.1). The whole Conda environment is exported to the file `environment.yml`, so, in theory, anyone should be able to get it running with a simple command:

```
$ conda env create -f environment.yml
```

Unfortunately, I encountered the following error stating that some libraries are incompatible:

```
Solving environment: failed

LibMambaUnsatisfiableError: Encountered problems while
   solving:
```

```
4   - package libopencv-4.5.3-py39h70bf20d_1 requires ffmpeg
        >=4.3.2,<4.4.0a0, but none of the providers can be
        installed
5
6 Could not solve for environment specs
7 The following packages are incompatible
8   - ffmpeg ==4.4.0 h6987444_5 is requested and can be
        installed;
9   - libopencv ==4.5.3 py39h70bf20d_1 is not installable
        because it requires
10      - ffmpeg >=4.3.2,<4.4.0a0 , which conflicts with any
            installable versions previously reported.
```

To resolve the problem, I tried manipulating versions of the conflicting libraries. But as a result, I always received even more errors.

To resolve the problem, I tried manipulating versions of the conflicting libraries but received even more errors. Therefore, I decided to build a compatible set of libraries from scratch as a Conda environment definition. I selected the same PyTorch and CUDA versions as in Section 4.3.1 and then fitted the rest of the dependencies. As a result, the following `environment.yml` file was created:

```
1  name: PlaneRecNet
2  channels:
3    - pytorch
4    - conda-forge
5    - nvidia
6    - defaults
7  dependencies:
8    - cffi=1.15.1
9    - cuda-toolkit=11.7
10   - numpy=1.21.2
11   - opencv=4.5.3
12   - pytorch::pytorch=1.13.1
13   - scipy=1.7.1
14   - pytorch::torchaudio=0.13.1
15   - pytorch::torchvision=0.14.1
16 prefix: $HOME/.conda/envs/PlaneRecNet
```

The final outcome is a one simple command setting the working environment for the PlaneRecNet:

```
1 $ conda env create -f environment.yml
```

4.4. Used Models Implementations

For plane segmentation comparison I used trained models shared by the articles' authors of both PlaneRCNN [43] and PlaneRecNet [49].

5. Results Evaluation

Hello, here is some text without a meaning. This text should show what a printed text will look like at this place. If you read this text, you will get no information. Really? Is there no information? Is there a difference between this text and some nonsense like "Huardest gefburn"? Kjift – not at all! A blind text like this gives you information about the selected font, how the letters are written and an impression of the look. This text should contain all letters of the alphabet and it should be written in of the original language. There is no need for special content, but the length of words should match the language.

5.1. Running state-of-the-art projects

Hello, here is some text without a meaning. This text should show what a printed text will look like at this place. If you read this text, you will get no information. Really? Is there no information? Is there a difference between this text and some nonsense like "Huardest gefburn"? Kjift – not at all! A blind text like this gives you information about the selected font, how the letters are written and an impression of the look. This text should contain all letters of the alphabet and it should be written in of the original language. There is no need for special content, but the length of words should match the language.

5.2. Model usefulness evaluation

Hello, here is some text without a meaning. This text should show what a printed text will look like at this place. If you read this text, you will get no information. Really? Is there no information? Is there a difference between this text and some nonsense like "Huardest gefburn"? Kjift – not at all! A blind text like this gives you information about the selected font, how the letters are written and an impression of the look. This text should contain all letters of the alphabet and it should be written in of the original language. There is no need for special content, but the length of words should match the language.

6. Conclusions and future works

In the past several years, there have been many possible uses for RGB-D-based technologies. However, most of them focus on detailed scanning like Honti et al. [50] with little use for simultaneous localization and mapping (SLAM). Resuming, the more progress in neural networks, the more the scientific community moves away from RGB-D in favor of plain RGB.

6.1. Achieved goals and observations

Hello, here is some text without a meaning. This text should show what a printed text will look like at this place. If you read this text, you will get no information. Really? Is there no information? Is there a difference between this text and some nonsense like “Huardest gefburn”? Kjift – not at all! A blind text like this gives you information about the selected font, how the letters are written and an impression of the look. This text should contain all letters of the alphabet and it should be written in of the original language. There is no need for special content, but the length of words should match the language.

6.2. Areas for development

Hello, here is some text without a meaning. This text should show what a printed text will look like at this place. If you read this text, you will get no information. Really? Is there no information? Is there a difference between this text and some nonsense like “Huardest gefburn”? Kjift – not at all! A blind text like this gives you information about the selected font, how the letters are written and an impression of the look. This text should contain all letters of the alphabet and it should be written in of the original language. There is no need for special content, but the length of words should match the language.

Bibliography

[1] Lizhi Zhang, Diansheng Chen, and Weihui Liu. "Fast plane segmentation with line primitives for RGB-D sensor". In: *International Journal of Advanced Robotic Systems* 13 (Dec. 2016), p. 172988141666584. DOI: 10.1177/1729881416665846.

[2] Tehreem Rabbani, F.A. Heuvel, and George Vosselman. "Segmentation of point clouds using smoothness constraint". In: *International Archives of Photogrammetry, Remote Sensing and Spatial Information Sciences* 36 (Jan. 2006).

[3] Bir Bhanu et al. "RANGE DATA PROCESSING: REPRESENTATION OF SURFACES BY EDGES." In: 1986. eprint: https://users.cs.utah.edu/~tch/publications/pub70.pdf. URL: https://api.semanticscholar.org/CorpusID:268107315.

[4] Angel Sappa and Michel Devy. "Fast range image segmentation by an edge detection strategy". In: vol. 0. Feb. 2001, pp. 292–299. ISBN: 0-7695-0984-3. DOI: 10.1109/IM.2001.924460.

[5] Rihua Xiang and Runsheng Wang. "Range image segmentation based on split-merge clustering". In: vol. 3. Sept. 2004, 614–617 Vol.3. DOI: 10.1109/ICPR.2004.1334604.

[6] X.Y. Jiang, U. Meier, and H. Bunke. "Fast range image segmentation using high-level segmentation primitives". In: *Proceedings Third IEEE Workshop on Applications of Computer Vision. WACV'96*. 1996, pp. 83–88. DOI: 10.1109/ACV.1996.572006.

[7] E. Natonek. "Fast range image segmentation for servicing robots". In: *Proceedings. 1998 IEEE International Conference on Robotics and Automation (Cat. No.98CH36146)*. Vol. 1. 1998, 406–411 vol.1. DOI: 10.1109/ROBOT.1998.676445.

[8] Yuichi Taguchi et al. "Point-plane SLAM for hand-held 3D sensors". In: May 2013, pp. 5182–5189. ISBN: 978-1-4673-5641-1. DOI: 10.1109/ICRA.2013.6631318.

[9] Martin A. Fischler and Robert C. Bolles. "Random sample consensus: a paradigm for model fitting with applications to image analysis and automated cartography". In: *Commun. ACM* 24.6 (June 1981), pp. 381–395. ISSN: 0001-0782. DOI: 10.1145/358669.358692. URL: https://doi.org/10.1145/358669.358692.

[10] Radu Rusu and Steve Cousins. "3D is here: Point cloud library (PCL)". In: May 2011. DOI: 10.1109/ICRA.2011.5980567.

[11] Renato Salas-Moreno et al. "Dense planar SLAM". In: Sept. 2014, pp. 157–164. DOI: 10.1109/ISMAR.2014.6948422.

[12] Michael Kaess. "Simultaneous localization and mapping with infinite planes". In: *Proceedings - IEEE International Conference on Robotics and Automation* 2015 (June 2015), pp. 4605–4611. DOI: 10.1109/ICRA.2015.7139837.

[13] Ming Hsiao et al. "Keyframe-based dense planar SLAM". In: May 2017, pp. 5110–5117. DOI: 10.1109/ICRA.2017.7989597.

[14] *Pinhole Camera Model*. https://hedivision.github.io/Pinhole.html. Accessed: 2024-09-21.

[15] *Point cloud*. https://en.wikipedia.org/wiki/Point_cloud. Accessed: 2024-09-21.

[16] Kai Arras and Roland Siegwart. "Feature Extraction and Scene Interpretation for Map-Based Navigation and Map Building". In: *Proceedings of SPIE, Mobile Robotics XII* 3210 (Aug. 1999). DOI: 10.1117/12.299565.

[17] Karl Pearson. "LIII. On lines and planes of closest fit to systems of points in space". In: *The London, Edinburgh, and Dublin Philosophical Magazine and Journal of Science* 2.11 (1901), pp. 559–572. DOI: 10.1080/14786440109462720. eprint: https://doi.org/10.1080/14786440109462720. URL: https://doi.org/10.1080/14786440109462720.

[18] Chen Liu et al. "PlaneNet: Piece-wise Planar Reconstruction from a Single RGB Image". In: (Apr. 2018). DOI: 10.48550/arXiv.1804.06278.

[19] Fisher Yu, Vladlen Koltun, and Thomas Funkhouser. "Dilated Residual Networks". In: July 2017, pp. 636–644. DOI: 10.1109/CVPR.2017.75.

[20] Jason Rambach et al. "SlamCraft: Dense Planar RGB Monocular SLAM". In: Mar. 2019. DOI: 10.23919/MVA.2019.8757982.

[21] Zehao Yu et al. "Single-Image Piece-Wise Planar 3D Reconstruction via Associative Embedding". In: June 2019, pp. 1029–1037. DOI: 10.1109/CVPR.2019.00112.

[22] Chen Liu et al. "PlaneRCNN: 3D Plane Detection and Reconstruction from a Single Image". In: (Dec. 2018). DOI: 10.48550/arXiv.1812.04072.

[23] Kaiming He et al. "Mask R-CNN". In: Oct. 2017, pp. 2980–2988. DOI: 10.1109/ICCV.2017.322.

[24] Yaxu Xie et al. "PlaneSegNet: Fast and Robust Plane Estimation Using a Single-stage Instance Segmentation CNN". In: Mar. 2021. DOI: 10.1109/ICRA48506.2021.9561693.

[25] Fangwen Shu et al. "Structure PLP-SLAM: Efficient Sparse Mapping and Localization using Point, Line and Plane for Monocular, RGB-D and Stereo Cameras". In: May 2023, pp. 2105–2112. DOI: 10.1109/ICRA48891.2023.10160452.

[26] Kurt Hornik, Maxwell Stinchcombe, and Halbert White. "Multilayer feedforward networks are universal approximators". In: *Neural Networks* 2.5 (1989), pp. 359–366. ISSN: 0893-6080. DOI: https://doi.org/10.1016/0893-6080(89)90020-8. URL: https://www.sciencedirect.com/science/article/pii/0893608089900208.

[27] Daniel Bolya et al. "YOLACT++: Better Real-time Instance Segmentation". In: *IEEE Transactions on Pattern Analysis and Machine Intelligence* PP (Aug. 2020), pp. 1–1. DOI: 10.1109/TPAMI.2020.3014297.

[28] Kaiming He et al. "Deep Residual Learning for Image Recognition". In: June 2016, pp. 770–778. DOI: 10.1109/CVPR.2016.90.

[29] Tsung-Yi Lin et al. "Feature Pyramid Networks for Object Detection". In: July 2017, pp. 936–944. DOI: 10.1109/CVPR.2017.106.

[30] Chaoxu Guo et al. "AugFPN: Improving Multi-Scale Feature Learning for Object Detection". In: June 2020, pp. 12592–12601. DOI: 10.1109/CVPR42600.2020.01261.

[31] Wei Liu et al. "SSD: Single Shot MultiBox Detector". In: vol. 9905. Oct. 2016, pp. 21–37. ISBN: 978-3-319-46447-3. DOI: 10.1007/978-3-319-46448-0_2.

[32] Niels Salscheider. "FeatureNMS: Non-Maximum Suppression by Learning Feature Embeddings". In: Jan. 2021, pp. 7848–7854. DOI: 10.1109/ICPR48806.2021.9412930.

[33] Yaxu Xie et al. *PlaneRecNet: Multi-Task Learning with Cross-Task Consistency for Piece-Wise Plane Detection and Reconstruction from a Single RGB Image*. 2021. arXiv: 2110.11219 [cs.CV].

[34] *Ubuntu*. https://ubuntu.com/. Accessed: 2024-09-25.

[35] *Conda Documentation*. https://docs.conda.io/en/latest/. Accessed: 2024-09-24.

[36] *Python*. https://www.python.org/. Accessed: 2024-09-25.

[37] *CUDA Toolkit*. https://developer.nvidia.com/cuda-toolkit. Accessed: 2024-09-24.

[38] *PyTorch*. https://pytorch.org/. Accessed: 2024-09-24.

[39] *Intel Core i5-10400F Processor*. https://www.intel.com/content/www/us/en/products/sku/199278/intel-core-i510400f-processor-12m-cache-up-to-4-30-ghz/specifications.html. Accessed: 2024-09-25.

[40] *GeForce RTX 4060 Family*. https://www.nvidia.com/en-us/geforce/graphics-cards/40-series/rtx-4060-4060ti/. Accessed: 2024-09-25.

[41] *Internal SSD 990 PRO*. https://semiconductor.samsung.com/consumer-storage/internal-ssd/990-pro/. Accessed: 2024-09-25.

[42] *CCamera FV-5 Samsung Galaxy A54 5G*. https://www.camerafv5.com/devices/manufacturers/samsung/scg21_scg21_0/. Accessed: 2024-09-24.

[43] *PlaneRCNN: 3D Plane Detection and Reconstruction from a Single Image*. https://github.com/NVlabs/planercnn. Accessed: 2024-09-24.

[44] *C language*. https://en.cppreference.com/w/c/language. Accessed: 2024-09-24.

[45] *C++ language*. https://en.cppreference.com/w/cpp/language. Accessed: 2024-09-24.

[46] *JIT Compiler, Faster Distributed, C++ Frontend*. https://github.com/pytorch/pytorch/releases/tag/v1.0.0. Accessed: 2024-09-26.

[47] *WeihongPan for of planercnn*. https://github.com/WeihongPan/planercnn-pytorch1.10.1_cuda11.3/tree/cuda11.3_pytorch1.10. Accessed: 2024-09-24.

[48] *RoIAlign for PyTorch*. https://github.com/longcw/RoIAlign.pytorch. Accessed: 2024-09-24.

[49] *PlaneRecNet*. https://github.com/EryiXie/PlaneRecNet. Accessed: 2024-09-24.

[50] Richard Honti, Ján Erdélyi, and Alojz Kopacik. "Semi-Automated Segmentation of Geometric Shapes from Point Clouds". In: *Remote Sensing* 14 (18) (Sept. 2022). DOI: 10.3390/rs14184591.